

# Changes of Proliferation Kinetics after X-Irradiation of a Human Malignant Melanoma Grown in Nude Mice\*

MOGENS SPANG-THOMSEN†‡ and LARS L. VINDELØV§

†University Institute of Pathological Anatomy, University of Copenhagen and §The Finsen Institute, Medical Department, Copenhagen, Denmark

**Abstract**—A human malignant melanoma grown in nude mice was exposed to single-dose X-irradiation and the effect on the proliferation kinetics was investigated by two methods. Flow cytometric DNA analysis was performed on tumour tissue obtained by sequential fine-needle aspirations after the treatment to monitor the initial cell cycle distribution changes. The technique of labelled mitoses was used to examine the kinetics of the tumours during regrowth. The results showed that the treatment initially induced a partial synchronization of small fractions of cells accumulated in the  $G_2$  phase of the cell cycle and a dose-dependent decrease of the cell generation time due to a shortening of the  $G_1$  duration time during regrowth of the tumours. Furthermore, it was shown that the calculated values of growth fraction and cell loss factor became unreliable because the tumours contained a dose-related increasing proportion of radiation-inactivated tumour cells.

## INTRODUCTION

THE CELL proliferation kinetics are important in the tumour response to radiotherapy, because the cellular sensitivity is dependent on the position in the cell cycle [1,2]. The recognition of the significance of proliferation kinetics and of treatment-induced changes of the parameters is mainly based on results from the study of experimental tumours and *in vitro* cultured cell lines [1-5].

The use of immune-deficient animals enables systematic *in vivo* studies of the cell kinetics of human tumours, and since basic tumour characteristics are preserved after heterotransplantation [6] the results obtained in the model system may be relevant for similar tumours in patients.

In this study a human malignant melanoma grown in nude mice was exposed to different single doses of X-irradiation. The initial radiation-induced kinetic changes were monitored by flow cytometric DNA analysis (FCM), and the regrowth kinetics of the tumour were investigated by the technique of labelled mitoses (PLM).

The FCM results showed that the treatment induced a generally dose-dependent partial synchronization of small fractions of cells accumulated in the  $G_2$  phase of the cell cycle, and the PLM results showed a dose-dependent decrease in the cell generation time due to shortening of the  $G_1$  duration time during regrowth of the tumours. The experimental data were used to estimate the growth fraction and the cell loss factor, but increasing proportions of radiation-inactivated tumour cells with dose made the calculated values unreliable for the treated tumours.

## MATERIALS AND METHODS

### *Tumour transplantation*

A tumour block of about 2 mm of a human malignant melanoma [7] was transplanted subcutaneously to each flank of 6-week-old female nude mice (BALB/c nu/nu BOM). The animals

Accepted 19 December 1983.

\*This study was supported by grants from the Danish Cancer Society, The A. Thaysen Foundation for Basic Medical Research, The Lundbeck Foundation, The Danish Medical Research Council, and The Danish Hospital Foundation for Medical Research, Region of Copenhagen.

‡To whom correspondence and requests for reprints should be addressed at: The University Institute of Pathological Anatomy, University of Copenhagen, 11, Frederik V's Vej, DK-2100 Copenhagen, Denmark.

were kept under sterile conditions in laminar clean benches. Room temperature was  $25 \pm 2^\circ\text{C}$ . Relative humidity was  $55 \pm 5\%$ . Sterile food pellets and water were given *ad libitum*.

In this study a total of 216 tumours in passages 49, 56, and 76 in nude mice were transplanted into 108 animals. Seventeen tumours were excluded: 14 because the mice died before the end of the experiments and three because the tumours showed no growth.

The mice were randomized to the treatment groups at the time of transplantation.

#### *Irradiation and dosimetry*

Three weeks after transplantation one tumour in each animal was irradiated. The tumours in the opposite flank of the mice served as controls [7]. A single dose X-irradiation of 0.7, 2.8, 7.4, 14.5 or 36.4 Gy was given under general anaesthesia and under sterile conditions as described previously [7], using a Müller RT 100 therapeutic unit, which yields 10.9 Gy/min at 100 kV, 8 mA, and with a 1.7-mm Al filter. The doses stated are calculated doses at the centre of 10-mm-diameter tumours.

#### *FCM analysis*

Tumour tissue for DNA analysis was obtained by fine-needle aspirations. The analyses were performed at intervals until 10 days after the irradiation. Following the last aspiration the tumours were labelled for PLM analysis (see below). On the tumours treated with 0.7 Gy, however, the FCM and PLM experiments were performed in separate series.

One treated and the untreated control tumour in the opposite flank of the mouse were aspirated for each time point and dose level. A total of 77 treated tumours and 77 untreated controls were aspirated. Individual tumours were biopsied only once.

The aspiration procedure, staining by propidium iodide and storage of samples were performed as described elsewhere [8–10]. The flow cytometer used was a cytofluorograph model 4802 (Bio/Physics System, Inc., Mahopac, NY) or a FACS III cell sorter (Becton Dickinson, Sunnyvale, CA). The DNA distributions were analysed by a computer program calculating the fractions of cells in the cell cycle phases [11].

#### *PLM analysis*

Ten days after irradiation, when regrowth had commenced in all dose-groups [7], the mice were given 40  $\mu\text{Ci}$   $^3\text{H}$ -labelled thymidine i.p. (sp. act. 6.7 Ci/mM, New England Nuclear). At intervals after the labelling the tumours were excised and immediately fixed in 4% neutral formaldehyde.

The tumours were cut into halves and 4- $\mu\text{m}$  sections were placed on rinsed slides. Using a dipping technique, the slides were coated with Kodak K-2 photoemulsion. After 6 weeks of exposure in the dark at  $4^\circ\text{C}$  the autoradiographs were developed in amidole, fixed in sodium thiosulphate and stained with haematoxylin. Using an oil-emersion objectives ( $\times 100$ ) and an ocular grid, at least 100 labelled and unlabelled mitoses were scored in representative areas of the tumours and the PLM (labelled mitoses/labelled + unlabelled mitoses  $\times 100$ ) was calculated.

In some of the irradiated tumours, however, the areas of surviving tumour tissue in the autoradiographs were so small that only 40–60 mitoses could be scored.

The background labelling of tumour cells in sections from unlabelled tumours were 0–2 grains. Mitoses labelled by four or more grains therefore were considered labelled.

A total of 165 tumours were prepared for PLM analysis, but 15 were excluded because the autoradiographs were unsuccessful.

The PLM data were analysed by a computer program [12] calculating the duration of the postmitotic phase ( $T_{G_1}$ ), of the DNA synthesis phase ( $T_S$ ), of the premitotic phase ( $T_{G_2}$ ) and of the median cell generation time ( $T_C$ ), together with the frequency distribution of  $T_C$ .

#### *Derived parameters*

The tumour volume doubling time was calculated according to

$$T_D = -\frac{1}{\alpha} \ln \left\{ 1 + (\ln 2 / \ln \frac{V(t)}{V(\max)}) \right\},$$

which was derived from the Gompertz growth function [13, 14]. In this equation  $V(t)$  is the volume at time  $t$ ,  $V(\max) = 12.683 \text{ mm}^3$  [14] is the theoretical maximum volume of this melanoma and  $\alpha$  is a constant. In this study  $T_D$  was calculated for  $V(t) = 200 \text{ mm}^3$ , applying the previously found values for  $\alpha$  in the individual treatment groups [7].

The potential doubling time was calculated from [15]:

$$T_{\text{pot}} = \lambda \frac{T_S}{LI}$$

and

$$\lambda = \frac{T_{\text{pot}}}{T_S} \left[ \exp \left\{ \frac{\ln 2}{T_{\text{pot}}} (T_{G_2} + T_S) \right\} - \exp \left\{ \frac{\ln 2}{T_{\text{pot}}} T_{G_1} \right\} \right].$$

In the calculations of  $T_{\text{pot}}$  the thymidine labelling index ( $LI$ ) was substituted by the S-phase fraction determined by FCM [16].

From the values of  $T_D$  and  $T_{\text{pot}}$  the cell loss factor was calculated [17]:

$$\phi = 1 - \frac{T_{\text{pot}}}{T_D}$$

The potential doubling time and the cell generation time ( $T_C$ ) were used for calculating the growth fraction from

$$\ln a = \frac{T_C}{T_{\text{pot}}} \ln 2$$

and

$$GF = a - 1,$$

where  $a$  is the number of proliferating cells produced per division [17].

## RESULTS

The results of the FCM analyses are shown in Fig. 1. Despite some variation in the results from individual tumours, it appears that the treatment generally caused dose-dependent changes in the cell cycle distribution. The changes between days 0 and 5 in the  $G_2 + M$  phase showed two elevations at an interval of 1.5–2 days. A maximum of about 20% of the cells were accumulated in this phase, corresponding to 3–5 times that of the control values. The first  $G_2 + M$  wave occurred at a dose-related interval after the treatment. Similar changes were seen in the S phase, with a delay of approximately 1 day. The  $G_1$  phase generally showed changes inverse to the  $G_2 + M$  phase.

After 5–8 days the cells had redistributed. With increasing dose the tumours redistributed to decreased  $G_1$  (and S) fractions and to an increased  $G_2 + M$  fraction compared to the pretreatment values (Fig. 1).

The cell distribution changes in the 36.4 Gy dose-group were less distinct (Fig. 1). The reason for this phenomenon is probably that large doses of irradiation result in a large fraction of radiation-induced necrotic cells. Therefore the cell cycle changes of the surviving cells are obscured in the FCM histograms.

Figure 2 shows the PLM data and the computed best-fitted curves, and it appears that the treatment caused a dose-dependent decreased distance between the two waves of labelled mitoses. The computed cell cycle duration times are listed in Table 1 together with the calculated kinetic parameters. The cell generation time  $T_C$

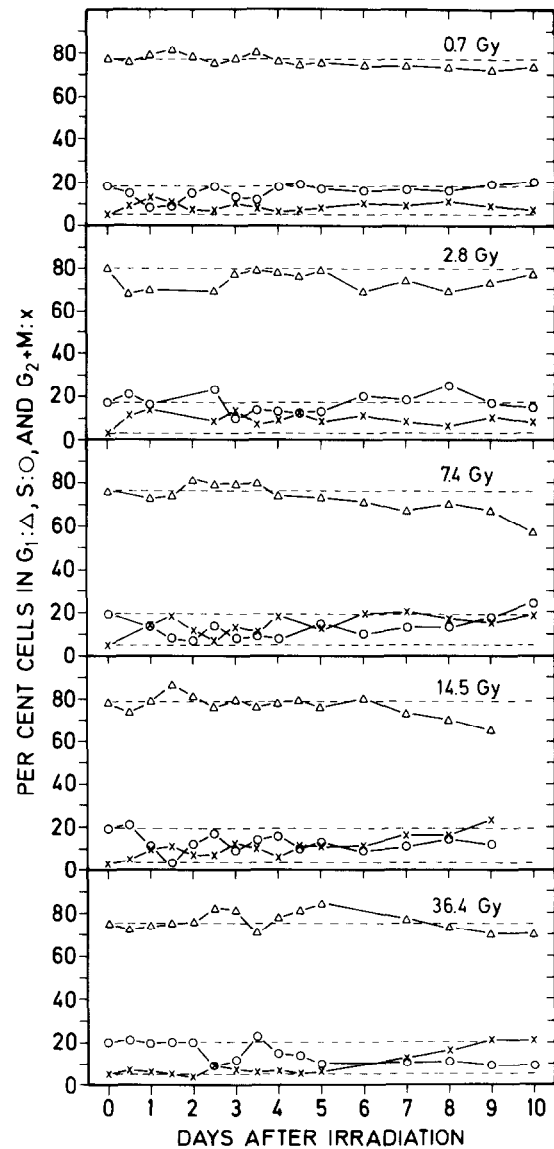


Fig. 1. Radiation-induced changes of the cell cycle distribution of a human malignant melanoma grown in nude mice. Flow cytometric DNA analysis was performed on tumour tissue obtained by fine-needle aspirations at intervals after irradiation on day 0 with the doses given in the figure. The data points are results from individual tumours. The cell cycle fractions plotted on day 0 and the corresponding broken lines represent means of the analysed control tumours.

decreased with dose from 40.8 (mean of the controls) to 27.6 hr after 36.4 Gy. The  $T_C$  decrease was due to a shortening of the  $G_1$  duration time, whereas no significant changes occurred in  $T_C$  and  $T_S$  (Table 1). Furthermore, the frequency distributions of the cell generation times (Fig. 3), which were drawn on the basis of the computer data of the PLM analysis [12], illustrate that the changes of  $T_C$  were caused by a narrowing of the distributions together with a minor displacement of the distributions towards smaller  $T_C$  values.

In addition to the  $T_C$  shortening, the irradiation apparently (see Discussion) caused a dose-dependent increase in the cell loss factor and

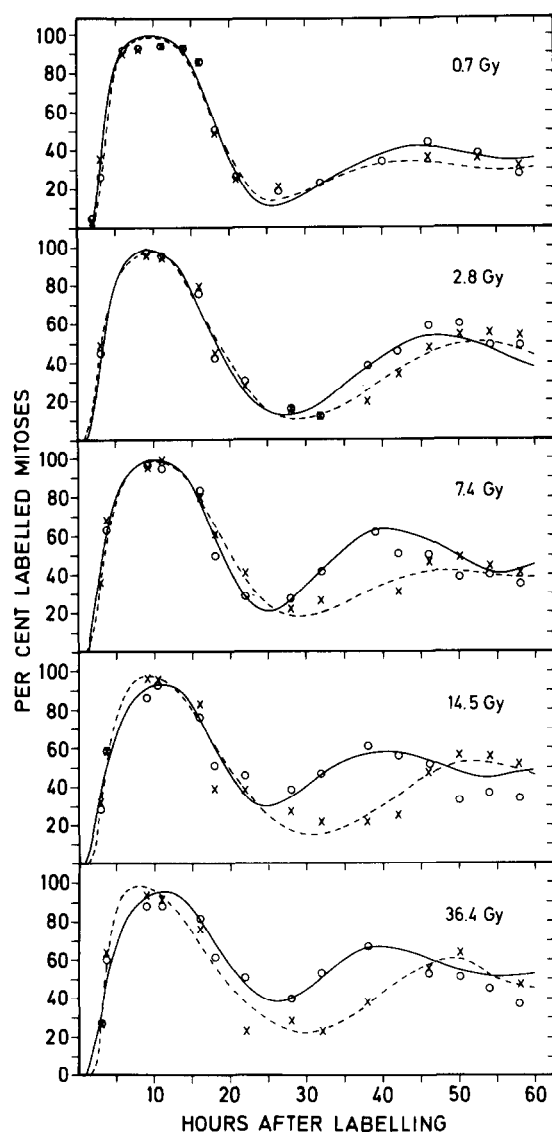


Fig. 2. Fractions of labelled mitoses after [ $^3\text{H}$ ]-thymidine pulse labelling of a human malignant melanoma grown in nude mice. The tumours were labelled 10 days after irradiation with the doses given in the figure. Data points from individual tumours and the computed best-fitted curves are shown for treated ( $\circ$  and solid lines) and untreated control tumours ( $\times$  and broken lines).

a simultaneous decrease in the growth fraction (Table 1).

## DISCUSSION

The present results have shown that single-dose irradiation in this human melanoma induced a partial synchronization of small fractions of cells and, following redistribution on days 5–8 after the treatment, a dose-dependent reduction of the cell generation time due to a shortening of the  $G_1$  duration time of the regrowing tumours.

The time interval between the FCM monitored  $G_2 + M$  accumulations (Fig. 1), which indicates an initial postirradiation generation time of 1.5–2 days, and the small fractions of synchronized

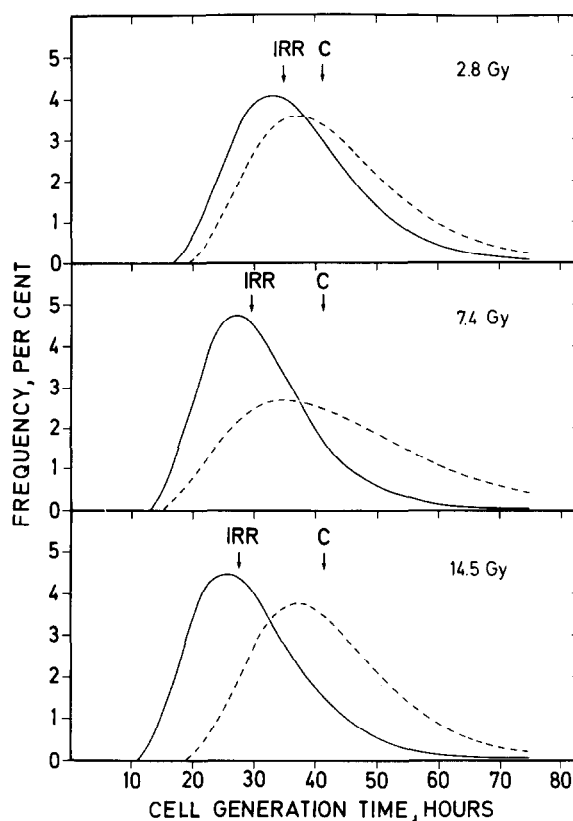


Fig. 3. Distributions of the cell generation times of a human malignant melanoma grown in nude mice. The distributions are consistent with the labelled mitoses data of Fig. 2 and Table 1. The computed median generation times are indicated by the arrows.

cells, reflecting the radiation-induced mitotic inhibition, are in agreement with previous results obtained with this tumour by determination of the changes in the mitotic index after irradiation [18]. It is questionable whether cell accumulation of this magnitude could be utilized in the design of fractionated radiotherapy to increase the treatment effect.

The PLM investigation of untreated tumours has shown [19] that the  $T_C$  of this tumour increased with increasing tumour size and that this  $T_C$  increase was caused by lengthening of the  $G_1$  duration time, whereas no significant changes occurred in the  $T_G$  and  $T_S$ . Since the volume of the surviving part of the tumours was reduced with the radiation dose [7], the dose-dependent  $T_C$  reduction due to shortening of the  $G_1$  duration time (Table 1) was to be expected. Furthermore, the results are in agreement with the PLM results of another human melanoma grown in nude mice [20].

The decreased  $T_G$  with dose (Table 1) correlates with the FCM results after redistribution, the  $G_1$  fraction generally demonstrating a dose-related decrease (Fig. 1).

The frequency distributions of the cell generation times of the regrowing tumours

Table 1. Proliferation characteristics of a human heterotransplanted malignant melanoma after single-dose irradiation

	* $T_C$ (hr)	$T_{G_2}$ (hr)	$T_S$ (hr)	$T_{G_1}$ (hr)	† $F_S$ (%)	‡ $T_D$ (days)	$\lambda$	$T_{pot}$ (hr)	$\phi$ (%)	$a$	$GF$ (%)
0.7 Gy	38.4	3.7	14.8	17.7	18.2	ND	0.78	63.4	—	1.52	52.1
Control	41.8	3.8	14.6	20.3	17.7	6.3	0.78	64.3	57.6	1.57	56.9
2.8 Gy	36.7	3.4	14.6	17.0	18.7	8.9	0.78	60.9	71.4	1.52	51.8
Control	41.4	3.2	15.1	20.9	16.6	6.3	0.77	70.0	53.9	1.51	50.6
7.4 Gy	29.6	3.3	15.2	9.4	18.2	9.6	0.78	65.1	71.6	1.37	37.0
Control	41.4	3.4	16.2	18.8	18.8	6.3	0.78	67.2	55.7	1.53	53.3
14.5 Gy	27.7	3.8	14.5	7.3	12.8	20.0	0.76	86.1	82.1	1.25	25.0
Control	41.3	3.7	15.7	19.7	19.2	6.3	0.79	64.6	57.4	1.56	55.8
36.4 Gy	27.6	3.7	15.8	5.9	9.6	101.5	0.74	121.8	95.0	1.17	17.0
Control	38.0	3.6	15.7	16.9	20.1	6.3	0.79	61.7	59.3	1.53	53.1

\*Computed median cell generation time ( $T_C$ ) and median duration times of the  $G_2$ , S and  $G_1$  phases of the cell cycle.

†Fraction of cells in the S phase of the cell cycle determined by flow cytometric DNA analysis. Control: mean S fraction of the analysed tumours. Treated tumours: mean S fraction of tumours analysed 8–10 days after treatment.

‡The tumour volume doubling time  $T_D$ , the proportionality constant  $\lambda$ , the potential doubling time  $T_{pot}$ , the cell loss factor  $\phi$ , the number of proliferating cells produced per division  $a$  and the growth fraction  $GF$  were calculated as described in Materials and Methods. ND: not done.

(Fig. 3) showed that the  $T_C$  shortening was mainly caused by a narrowing of the distributions. The change may thus be interpreted as a dose-dependent decrease in the kinetic heterogeneity of the surviving tumour cells. This may implicate an advantage in the planning of fractionated radiotherapy or combined treatment with cell cycle phase-specific drugs, because the cell cycle fractions of the treated tumours obtained by FCM will represent kinetically more homogeneous cell populations than those of untreated tumours.

The study of experimental tumours and *in vitro* cultured cells have shown that radiation-inactivated cells may pass through several cell cycles before they die [21]. The increase in the  $G_2 + M$  fraction (Fig. 1) on days 6–10, especially after applying the higher doses, may thus represent doomed cells that have lost their ability of division but have still not disintegrated.

In a previous study it was found that single-dose irradiation induced a dose-dependent decrease in the regrowth rate of this tumor [7]. This is apparently inconsistent with the present PLM results, demonstrating a dose-dependent increase in the proliferation rate during regrowth. However, it was also found that the amount of necrosis increased with increasing dose [7]. Hence with increasing dose the necrotic masses grew, thereby causing a reduction of the proportion of surviving tumour tissue. This resulted in the dose-dependently decreased net growth rate, even though the proliferation rate was dose-dependently increased.

The calculated cell loss factor ( $\phi$ ) of the treated

tumours increased with dose (Table 1). This is in agreement with the results from single-dose irradiated experimental tumours [22]. However, the investigations of untreated tumours of different size [19] showed that the  $\phi$  of this melanoma increased with increasing tumour volume. It was thus to be expected that  $\phi$  would decrease with dose, since the volume of the surviving tumour tissue decreased with dose [7]. The discrepancy between the observed increase and the expected decrease in  $\phi$  can be explained by the increasing necrosis with dose. If the growth of unperturbed tumours involves the formation of an increasing necrotic proportion, the necrosis will add to the measured volume and cause a decrease in the volume doubling time. The use of  $T_D$  will then tend to underestimate the cell loss factor [15]. The increasing necrotic proportion of the tumours in the present investigation, however, was not produced as a result of proliferation, and was thus related to the surviving cell population 'pre-existing'. Therefore the radiation-induced necrosis caused a dose-dependent *increase* in the tumour volume doubling time (Table 1), and the use of  $T_D$  in this case caused an *overestimation* of the cell loss factor.

In the investigation of untreated tumours [19] it was found that the growth fraction showed no systematic changes during tumour growth. Therefore no changes due to treatment-induced reduction of tumour volume was to be expected in the growth fraction of the irradiated tumours. This is apparently inconsistent with the decreas-

ing values with dose in growth fraction of the treated tumours (Table 1). However, the increasing fraction of doomed  $G_2 + M$  cells with dose (Fig. 1) resulted in underestimated S phase fractions (Table 1) which would also have been found by use of conventional determination of thymidine labelling index, since doomed cells are unrecognizable from the surviving cells. Thus the use of the underestimated S fractions caused an overestimation of  $T_{pot}$  and thereby the decreasing values with dose in the growth fraction of the treated tumours (Table 1).

It may thus be concluded that in tumours demonstrating undisturbed macroscopic regrowth,

calculation of the cell loss factor and the growth fraction may provide unreliable and misleading results when the measured volume in addition to the growing tumour contains a substantial proportion of radiation-inactivated cells.

**Acknowledgements**—The authors are indebted to Dr Gordon G. Steel for performing the computer analysis of the PLM data. We thank cand. act. A. Nielsen and Mr I. J. Christensen for statistical assistance, and the excellent technical assistance of Mrs C. Holstein, Miss E. Højgaard Thomsen, Mrs V. Hornhaver, Miss L. E. Christiansen and Miss E. Høj is gratefully acknowledged.

## REFERENCES

1. Sinclair WK. Cyclic X-ray responses in mammalian cells *in vitro*. *Radiat Res* 1968, **33**, 620–643.
2. Terasima T, Tolmach LJ. Changes in X-ray sensitivity of HeLa cells during the division cycle. *Nature* 1961, **190**, 1210–1211.
3. Dethlefsen LA. Cellular recovery kinetic studies relevant to combined-modality research and therapy. *Int J Radiat Oncol Biol Phys* 1979, **5**, 1197–1203.
4. Hermens AF, Barendsen GW. The importance of proliferation kinetics and clonogenicity of tumor cells for volume responses of experimental tumors after irradiation. In: Nygaard OF, Adler HI, Sinclair WK, eds. *Proceedings of the 5th International Congress on Radiation Research*. New York, Academic Press, 1975, 834–849.
5. Withers HR. The four R's of radiotherapy. In: Lett JT, Adler H, eds. *Advances in Radiation Biology*. New York, Academic Press, 1975, Vol. 5, 241–271.
6. Povlsen CO, Visfeldt J, Rygaard J, Jensen G. Growth patterns and chromosome constitution of human malignant tumours after long-term serial transplantation in nude mice. *Acta Pathol Microbiol Scand (A)* 1975, **83**, 709–716.
7. Spang-Thomsen M, Visfeldt J, Nielsen A. Effect of single dose X irradiation on the growth curves of a human malignant melanoma transplanted into nude mice. *Radiat Res* 1981, **85**, 184–195.
8. Vindeløv LL, Christensen IJ, Keiding N, Spang-Thomsen M, Nissen NI. Long-term storage of samples for flow cytometric DNA analysis. *Cytometry* 1983, **3**, 317–322.
9. Vindeløv LL, Christensen IJ, Nissen NI. A detergent-trypsin method for the preparation of nuclei for flow cytometric DNA analysis. *Cytometry* 1983, **3**, 323–327.
10. Vindeløv LL, Christensen IJ, Nissen NI. Standardization of high-resolution flow cytometric DNA analysis by the simultaneous use of chicken and trout red blood cells as internal reference standards. *Cytometry* 1983, **3**, 328–331.
11. Christensen IJ, Hartmann NR, Keiding N, Larsen JK, Noer H, Vindeløv L. Statistical analysis of DNA distributions from cell populations with partial synchrony. In: Lutz D, ed. *Pulse-cytophotometry*. Ghent, European Press Medicon, 1978, Vol. 3, 71–78.
12. Steel GG, Hanes S. The technique of labelled mitoses: analysis by automatic curve-fitting. *Cell Tissue Kinet* 1971, **4**, 93–105.
13. Gompertz B. On the nature of the function expressive of the law of human mortality, and on a new mode of determining the value of life contingencies. *Phil Trans R Soc London (B)* 1825, **115**, 513–585.
14. Spang-Thomsen M, Nielsen A, Visfeldt J. Growth curves of three human malignant tumors transplanted to nude mice. *Exp Cell Biol* 1980, **48**, 138–154.
15. Steel GG. Cell loss from experimental tumours. *Cell Tissue Kinet* 1968, **1**, 193–207.
16. Rofstad EK, Fodstad Ø, Lindmo T. Growth characteristics of human melanoma xenografts. *Cell Tissue Kinet* 1982, **15**, 545–554.
17. Steel GG. Cell loss as a factor in the growth rate of human tumours. *Eur J Cancer* 1967, **3**, 381–387.
18. Spang-Thomsen M, Visfeldt J. Growth curves and radiation-induced synchronization of a human malignant melanoma transplanted to nude mice. In: Nomura T, Ohsawa N, Tamaoki N, Fujiwara K, eds. *Proceedings of the 2nd International Workshop on Nude Mice*. Tokyo, University of Tokyo Press, 1977, 327–336.

19. Spang-Thomsen M, Vindeløv LL. Proliferation kinetics of a human malignant melanoma serially grown in nude mice. *Cell Tissue Kinet* In press.
20. Rofstad EK, Lindmo T, Brustad T. Effect of single dose irradiation on the proliferation kinetics in a human malignant melanoma in athymic nude mice. *Acta Radiol Oncol Radiat Phys Biol* 1980, 19, 261-269.
21. Okada S. Radiation-induced death. In: Altman KI, Gerber GB, Okada S, eds. *Radiation Biochemistry*. New York, Academic Press, 1970, Vol. 1, 247-307.
22. Denekamp J, Thomlinson RH. The cell proliferation kinetics of four experimental tumors after acute X-irradiation. *Cancer Res* 1971, 31, 1279-1284.